JIGAWA JOURNAL OF
ENVIRONMENTAL AND EARTH SCIENCES
Federal University Dutse | Department of Environmental Sciences

Volume 1 • Issue 1 • November 2026 ISSN: 3093-8852 ISSN Online: 3093-8842

ORIGINAL RESEARCH ARTICLE

Spatial assessment of physical factors influencing flood susceptibility along the Hadejia River axis, Jigawa State, Nigeria

Shehu Amina Ummi*, Shehu Nurudeen Muhammad and Dau Abba Umar

Department of Environmental Sciences, Faculty of Physical Sciences
Federal University Dutse, Jigawa State-Nigeria
Corresponding author: aushehuado@gmail.com; +234 703 903 5271

RECEIVED	ACCEPTED	PUBLISHED	DOI
11/09/2026	01/11/2026	02/11/2026	

How to cite: Shehu Amina Ummi, Shehu Nurudeen Muhammad and Dau Abba Umar (2026). Spatial assessment of physical factors influencing flood susceptibility along the Hadejia River axis, Jigawa State, Nigeria. *Jigawa Journal of Environmental and Earth Sciences*, 1(1), 53–69. https://doi.org/xx
Copyright and licence: © 2026 https://jijees.fud.edu.ng

ABSTRACT

Recurrent seasonal flooding along the Hadejia River basin poses severe threats to agricultural productivity, rural settlements, and regional food security in semi-arid northwestern Nigeria. This study models and delineates spatial flood susceptibility zones along a 0–5 km buffer axis of the Hadejia River and its primary tributaries across eight Local Government Areas (LGAs) in Jigawa State anchored by 23 farming communities and encompassing a verified spatial extent of 5,902.55 km^2. Utilizing Geographic Information System (GIS) and the Analytic Hierarchy Process (AHP), seven hydro-geomorphic and thematic conditioning factors were evaluated: ALOS PALSAR 12.5m Digital Elevation Model (DEM)-derived elevation and slope, 10-year (2011–2020) meteorological records of mean annual rainfall interpolated via Inverse Distance Weighting (IDW), ISRIC 250m soil hydraulic conductivity data, Landsat 8 Operational Land Imager (OLI) Land Use/Land Cover (LULC), drainage density and Euclidean distance to the active river channel. Criteria were structured into a five-criterion pairwise comparison matrix with verified mathematical consistency (λ_{max} = 5.2453, CI = 0.0613, CR = 0.0547 < 0.10). The expert-derived criteria weights were verified to ensure complete accounting across all five criteria with mean annual rainfall (46.66%), distance to river and drainage density (26.86%), slope and elevation (16.97%), soil type (4.76%) and land use/land cover (4.76%). Through weighted raster overlay, the river axis was classified into three susceptibility zones using Natural Breaks: High Susceptibility (37.02%, 2,185.34 km^2), Moderate Susceptibility (41.06%, 2,423.82 km^2) and Low Susceptibility (21.92%, 1,293.39 km^2). High-susceptibility zones are strongly concentrated in low-lying downstream floodplains (337–365 m) characterized by flat terrain (0.0°–1.33°), poorly drained clayey fluvisols and immediate channel proximity (<1 km), primarily encompassing Guri, Hadejia, Auyo and southern Kirikasama LGAs. This physical terrain model provides baseline spatial evidence for targeted environmental zoning, drainage optimization and pre-disaster planning, addressing key methodological and reporting deficiencies in regional hazard assessments.

Keywords: Flood susceptibility mapping, Analytic Hierarchy Process (AHP), Multi-Criteria Decision Analysis, Hadejia River, Remote Sensing.

Introduction

Flooding is one of the most frequent, pervasive, and economically devastating natural hazards worldwide, accounting for approximately 47% of all weather-related disasters globally (Vishwanath & Tomaszewski, 2018). In arid and semi-arid river systems, seasonal

flood discharges routinely exceed the carrying capacities of natural drainage channels, inundating extensive floodplains, submerging standing crops, destroying rural infrastructure, and disrupting rural livelihoods (Alfa *et al*. 2018). Globally, climate-induced disasters generate economic losses exceeding billions of dollars annually (Swiss Re, 2020), with disproportionate impacts borne by agrarian communities where rural smallholders rely almost exclusively on riparian wetlands for recession farming and irrigation (Molinari *et al*. 2017).

In Nigeria, recurrent overbank flooding along major river networks has submerged millions of hectares of arable land and disrupted cereal and legume production across core agro-ecological zones (Anugwara & Emakpe, 2013). The Hadejia River basin in northwestern Nigeria represents a vital ecological and agricultural axis within the Sudano-Sahelian zone. Smallholder farming communities in Jigawa State depend extensively on the fertile alluvial floodplains for rainfed farming during the wet season and fadama irrigation of vegetables, wheat, and rice during the dry season. However, this critical agricultural belt experiences perennial and destructive flooding. Seasonal inundations—driven by intense monsoonal rains, natural sediment deposition, upstream reservoir releases from the Tiga and Challawa Gorge dams, and pervasive typha grass (Typha domingensis) siltation—routinely inundate settlements, destroy standing crops, and exacerbate regional food insecurity.

To establish a sound methodological framework, clear conceptual distinctions must be drawn among interrelated disaster terms. In natural hazard science, flood hazard refers to the physical occurrence, probability, depth, and velocity of inundation (European Commission, 2007). Flood susceptibility represents the intrinsic propensity or predisposition of a landscape to flood based on static or quasi-static hydro-geomorphic conditioning factors—such as elevation, slope gradient, soil hydraulic conductivity, and drainage network proximity—independent of transient weather events. Exposure denotes the inventory of human populations, dwellings, agricultural lands, and infrastructure located within the hazard zone. Vulnerability reflects the socio-economic, structural, or physical predisposition of exposed elements to suffer adverse effects when impacted. Consequently, total flood risk represents the convolution of hazard (or susceptibility), exposure, and vulnerability (Risk = Hazard × Exposure × Vulnerability). When detailed socio-economic vulnerability indicators and asset exposure inventories are not evaluated, geospatial analysis models physical flood susceptibility rather than holistic socio-economic risk.

Multi-Criteria Decision Analysis (MCDA) integrated with Geographic Information Systems (GIS) and remote sensing has become an established, computationally robust approach for evaluating flood susceptibility across data-scarce and ungauged river basins (Bello & Jeb, 2014; Rincón *et al*. 2018; Li *et al*. 2019). Among MCDA methodologies, the Analytic Hierarchy Process (AHP) formulated by Saaty (1980, 2008) provides a structured mathematical procedure for deriving criterion weights via pairwise comparisons while enforcing consistency verification through the Consistency Ratio (CR). Several studies have examined flooding within Jigawa State and the broader Lake Chad basin. Mahmoud & Gan (2018) applied multi-criteria GIS modeling across the Hadejia River Basin, emphasizing regional hydro-climatic variables. More recently, Shuaibu *et al*. (2022) and Shuaibu (2020) implemented a hydro-geomorphic approach, concluding that regional topographic controls—specifically elevation (33%) and slope (24%)—strongly dictate basin-wide

inundation patterns, whereas localized semi-arid floodplains often exhibit high sensitivity to precipitation depth and channel proximity (Kura *et al.* 2022).

While previous macro-scale studies have characterized the broader basin, there remains a critical need for high-resolution, axis-specific assessments that integrate ALOS PALSAR 12.5m terrain data to delineate local susceptibility gradients across the vulnerable farming settlements of the Hadejia River. The aim of this study is to model and delineate spatial flood susceptibility zones along the Hadejia River axis in Jigawa State using an integrated GIS and AHP multi-criteria framework. The specific objectives are to: (1) acquire, standardize and reclassify seven key hydro-geomorphic and environmental conditioning factors (elevation, slope, soil hydraulic conductivity, mean annual rainfall, drainage density, proximity to river channels and land use/land cover); (2) establish an AHP pairwise comparison matrix to derive objective criteria weights with verified mathematical consistency; (3) perform multi-criteria weighted raster overlay to produce a comprehensive flood susceptibility map; and (4) evaluate the spatial distribution of susceptibility classes across eight LGAs, anchored by 23 farming communities.

Study area

Geographic location, extent and regional hydrology

The study was conducted along the Hadejia River axis located in eastern Jigawa State, northwestern Nigeria. The Hadejia River represents a major drainage network within the semi-arid Lake Chad Basin. Originating from the granitic basement complex highlands of Kano State, the river flows northeastward through the flat sedimentary plains of Jigawa State, forming the ecologically significant Hadejia-Nguru Wetlands before converging with the Jama'are River to form the Yobe River system, which ultimately drains into Lake Chad. The entire Hadejia-Jama'are River Basin encompasses a catchment area of approximately 30,569 km^2 (Mahmoud & Gan, 2018).

Delineation of the river axis and the 23 farming communities

To evaluate fluvial overbank flooding where flood hazards directly intersect human habitations and farming activities, this investigation focused on a 0–5 km buffer axis along the main Hadejia River channel and its primary distributaries. The analysis extent traverses eight Local Government Areas (LGAs): Miga, Kaugama, Auyo, Kafin Hausa, Hadejia, Malam Madori, Guri, and Kirikasama. The axis boundary was established through Euclidean buffer delineation constrained by LGA boundaries, yielding a verified total extent of the study area to be 5,902.55 km^2 (590,255.12 hectares).

Within this 0–5 km buffer zone, 23 farming communities distributed across the eight LGAs were identified and mapped using handheld GPS receivers. These 23 communities represent the primary agricultural and settlement clusters situated across three distinct river-proximity zones (<3 km, 3–4 km, and 4.1–5 km), serving as geographic control points and ground-validation for the spatial modeling framework, as illustrated in the study area map (Figure 1) and community buffer distribution map (Figure 3).

Topography and geomorphology

Geomorphologically, the study axis forms an expansive, gently undulating plain underlain by sedimentary formations of the Chad Formation. The terrain exhibits a very gentle regional slope descending from southwest to northeast. Digital elevation data reveal that altitudes range from a maximum of 419m above mean sea level in the southwestern uplands of Miga and Kafin Hausa to a minimum of 337m in the extensive northeastern depression plains of Guri, Hadejia, and Kirikasama. Because of this exceptionally low topographic relief, river gradients are minimal, severely restricting channel conveyance and causing extensive overbank spilling during high-flow periods.

Climate, rainfall gradient and seasonality

The climate of the study area is semi-arid Sudano-Sahelian, characterized by two sharply contrasting seasons: a short-wet season lasting 4 to 6 months (typically May/June to October) and a prolonged dry season (November to April). The seasonal cycle is governed by the latitudinal oscillation of the Inter-Tropical Convergence Zone (ITCZ), which mediates the alternation between humid maritime South-West (SW) trade winds originating from the Atlantic Ocean and dry, dust-laden North-East (NE) continental trade winds blowing from the Sahara Desert. Mean annual rainfall varies spatially and temporally, spanning 349mm to 956mm across the axis. Precipitation exhibits a pronounced south-to-north decline, with southern LGAs (Miga, Kafin Hausa) receiving up to 956mm, while northeastern LGAs (Guri, Kirikasama) receive less than 470mm annually.

Land use and the smallholder agrarian economy

The Hadejia River axis is predominantly an agricultural landscape, with arable farmland and productive alluvial floodplains (fadama) comprising over 80% of the total land surface. Agriculture constitutes the primary livelihood of the population, with approximately 82% of inhabitants engaged as smallholder farmers operating family holdings under 2.5 hectares. Agrarian production is heavily reliant on rainfed cultivation of staple grains and legumes—including sorghum, millet, maize, cowpea, and groundnut—during the wet season. During the dry season, the alluvial wetlands support intensive recession farming and small-scale pump irrigation of rice, wheat, onions, tomatoes, and peppers. Consequently, seasonal overbank flooding along this river axis directly threatens rural livelihoods, agricultural capital, and regional food security.

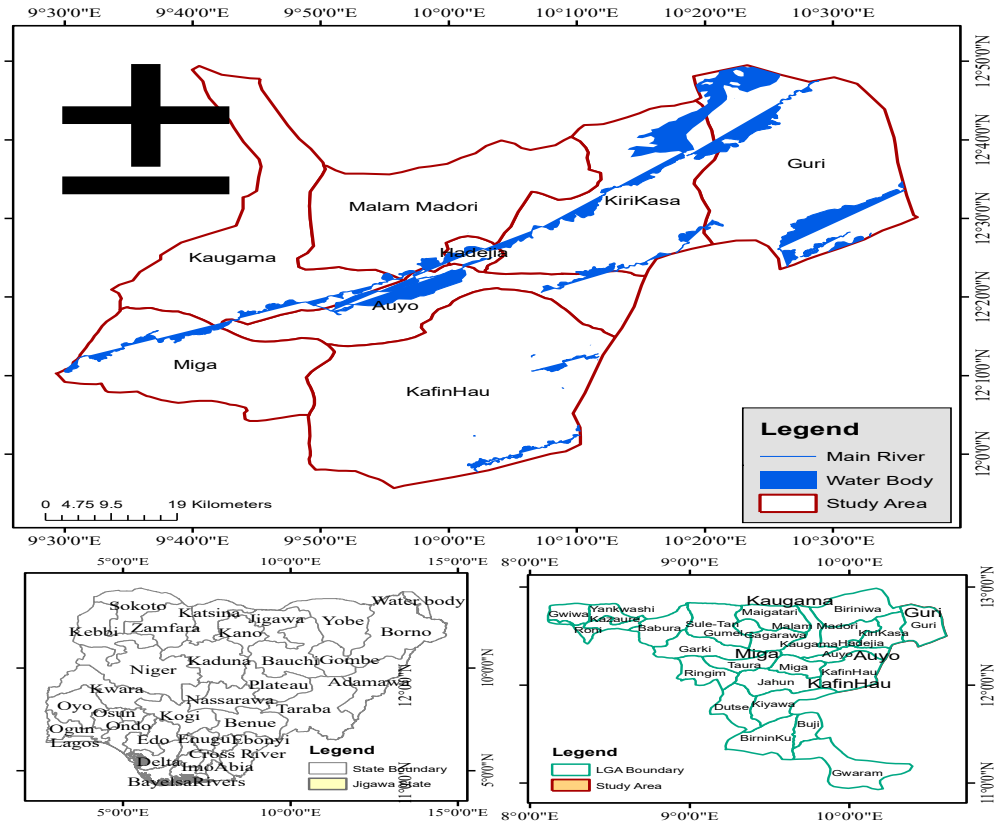


Figure 1: Map of Study area showing the eight LGAs

Department of Environmental Sciences, Federal University Dutse, 2020

Materials and methods

Software, instrumentation and geospatial processing environment

All spatial data processing, hydrologic conditioning, thematic raster standardization, multi-criteria weighting and spatial overlay modeling were performed in Environmental Systems Research Institute (ESRI) ArcGIS 10.8 utilizing the Spatial Analyst extension. Primary geographic coordinates and ground control points for the 23 farming communities were acquired during field surveys using a Garmin handheld Global Positioning System (GPS) receiver. Figure 2 illustrates the methodological workflow executed in this study.

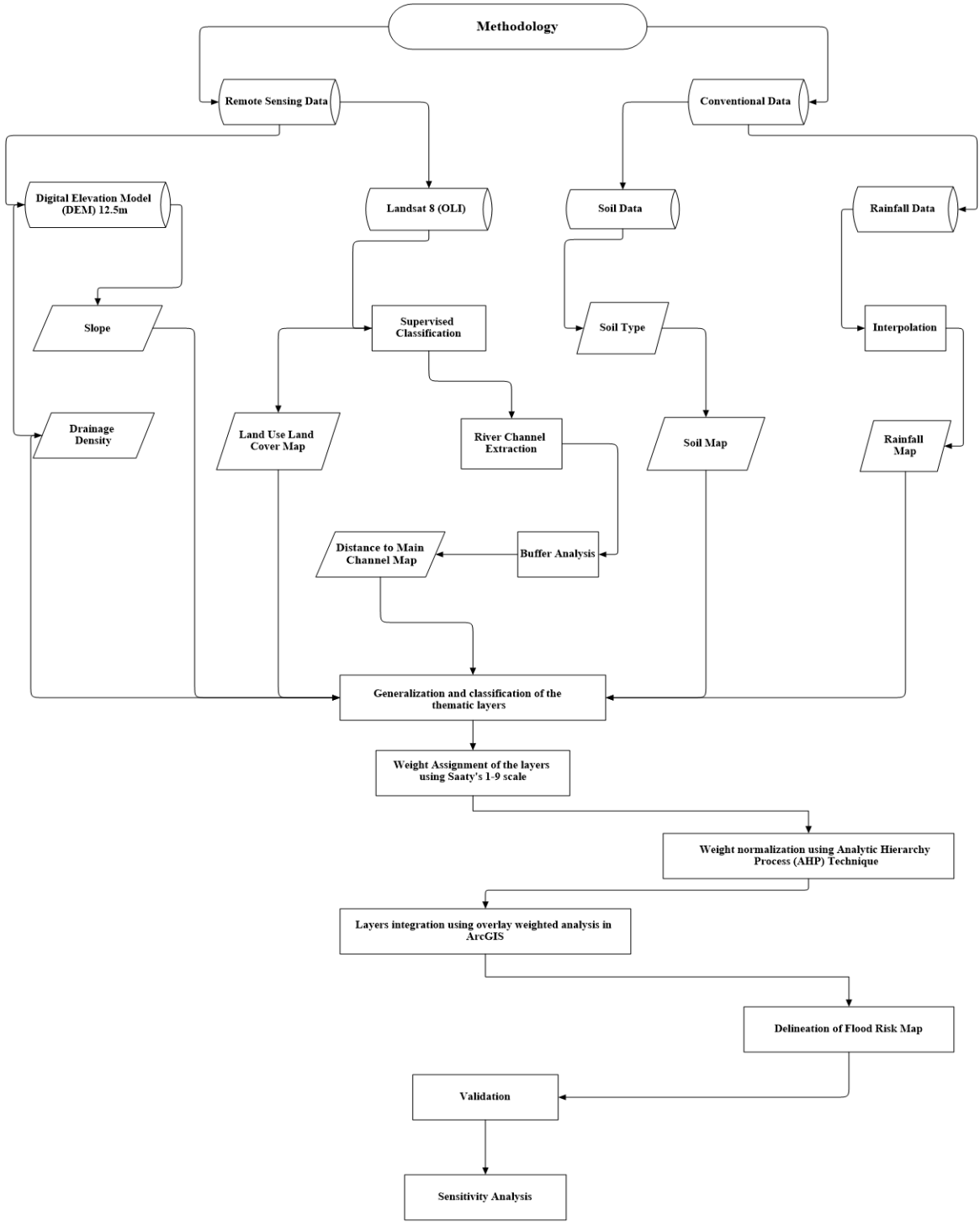


Figure 2: Methodological workflow for GIS-AHP-Based flood susceptibility assessment

Author's compilation, 2021

Spatial datasets and characteristics

The geospatial and hydro-climatic datasets utilized in this research, along with their acquisition sources, temporal spans and preprocessing routines are summarized in Table 1.

Table 1: Primary Spatial Datasets, Metadata and Hydro-Geomorphic Preprocessing Characteristics

Thematic Factor	Source/ Satellite Sensor	Temporal Extent	Spatial Resolution	Preprocessing & Methodological Treatment
Topography (Elevation & Slope)	ALOS PALSAR RTC DEM	2011	12.5m	Sink filling, slope calculation (degrees), reprojected to UTM 32N.
Precipitation (Mean Annual)	JARDA Meteorological Records	2011–2020 (10-yr mean)	Station points	Inverse Distance Weighted (IDW) interpolation.
Soil Properties & Texture	ISRIC World Soil Information	2020	250m	Clipped to boundary, categorized by hydraulic conductivity.
Drainage Network & Density	Derived from ALOS PALSAR DEM	Derived	12.5m cell	Hydro-conditioning, flow accumulation, Line Density (km/km^2).
Distance to River Channel	Derived Stream Network	Derived	Vector	Euclidean distance buffering (<1 km, 1–2, 2–3, 3–4, >4 km).
Land Use / Land Cover (LULC)	Landsat8 OLI/TIRS (Path 187, Row 51)	Nov,2020 (Dry season)	30m (resampled 12.5 m)	Supervised Maximum Likelihood Classification into 6 classes.

Author's Analysis, 2021

River axis delineation and community ground control

To establish an objective spatial domain, a 0–5 km buffer was delineated outward from the active river channel of the Hadejia River and its primary tributaries across the eight LGAs. Within this axis, farming communities were selected as representative geographic anchors across three proximity strata (<3 km, 3–4 km, and 4.1–5 km). Ground coordinates captured at these settlements were imported into the GIS environment to verify the spatial accuracy of the hydrographic and thematic layers, establish ground control for LULC classification, and contextualize local terrain conditions relative to historical flood occurrences (Figure 3).

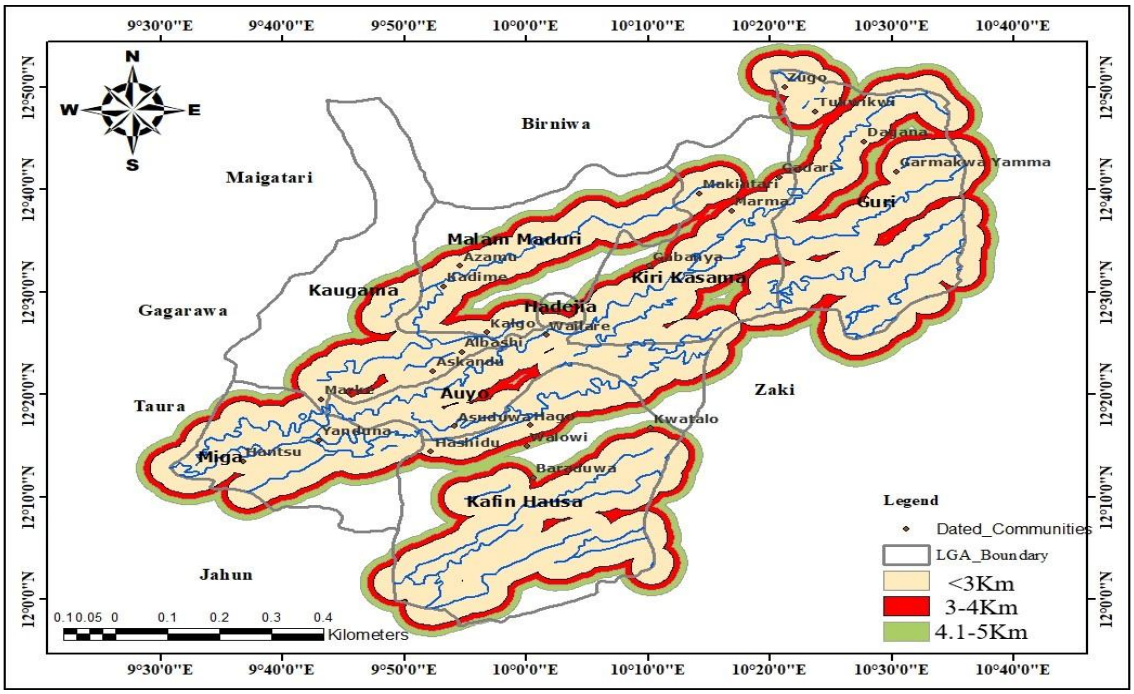


Figure 3: Buffer layer zone (0-5 km) and spatial Distribution of the 23 farming communities

Author's compilation, 2021

Hydro-geomorphic conditioning factors and standardization

Flood occurrence is conditioned by a complex interplay of topographic, hydrologic, pedologic and anthropogenic factors (Mishra & Sinha, 2020). Seven conditioning factors were processed, converted to raster format at a standardized 12.5 m cell resolution and reclassified onto a common 1 to 5 numerical scale representing flood susceptibility: 1 = Very Low, 2 = Low, 3 = Moderate, 4 = High, and 5 = Very High (Table 2).

a. Elevation: Low-elevation terrains act as regional sinks that collect overland runoff, whereas elevated interfluves promote gravitational drainage.

b. Slope: Slope gradient governs the velocity of overland flow. Gentle slopes impede surface runoff velocity and cause extensive ponding, whereas steep slopes accelerate gravitational discharge away from catchment divides.

c. Soil Type: Soil texture directly determines hydraulic conductivity and infiltration capacity. Poorly drained soils promote saturation excess overland flow, while porous soils absorb rainfall.

d. Mean Annual Rainfall: Precipitation provides the primary hydrologic volume driving surface runoff. Ten-year rainfall records (2011–2020) from the Jigawa Agricultural and Rural Development Authority (JARDA) were averaged and interpolated across the axis using Inverse Distance Weighting (IDW) to produce a continuous precipitation isohyet surface.

e. Drainage Density: Drainage density measures the total stream length per unit catchment area (km/km^2), generated using the Line Density tool. High drainage density signifies rapid hydrologic collection and intense surface runoff generation.

f. Distance to River: Proximity to active river channels is a primary determinant of fluvial overbank inundation. Multi-ring Euclidean distance buffers were created at 1 km intervals.

g. Land Use / Land Cover (LULC): Surface cover governs rainfall interception, infiltration, and surface roughness. Landsat 8 imagery was classified into six thematic categories: Shrubland, Farmland, Dense Vegetation, Built-up Areas, Water Bodies, and Bare Surfaces.

Table 2: Multi-Criteria Standardization and Reclassification Scheme for Conditioning Factors

Conditioning Criterion	Criterion Weight	Sub-Class Range	Susceptibility Score (1–5)	Hydrological / Geomorphic Justification
Mean Annual Rainfall	46.66%	349 – 470 mm 471 – 590 mm 591 – 710 mm 711 – 830 mm 831 – 956 mm	1 (Very Low) 2 (Low) 3 (Moderate) 4 (High) 5 (Very High)	Greater rainfall depth generates larger volume of surface runoff.
Distance to River Channel	13.43% (Shared 26.86%)	> 4.0 km 3.0 – 4.0 km 2.0 – 3.0 km 1.0 – 2.0 km < 1.0 km	1 (Very Low) 2 (Low) 3 (Moderate) 4 (High) 5 (Very High)	Riparian proximity dictates susceptibility to channel overtopping.
Drainage Density	13.43% (Shared 26.86%)	7.07 – 32.0 km/km^2 32.1 – 56.8 km/km^2 56.9 – 81.7 km/km^2 81.8 – 107.0 km/km^2 108.0 – 132.0 km/km^2	1 (Very Low) 2 (Low) 3 (Moderate) 4 (High) 5 (Very High)	High channel density reflects rapid surface runoff accumulation.
Slope Gradient	8.485% (Shared 16.97%)	> 11.5° 5.8° – 11.5° 3.1° – 5.7° 1.4° – 3.0° 0.00° – 1.33°	1 (Very Low) 2 (Low) 3 (Moderate) 4 (High) 5 (Very High)	Low gradients impede runoff velocity, promoting surface ponding.
Elevation (Altitude)	8.485% (Shared 16.97%)	399 – 419 m 381 – 398 m 366 – 380 m 351 – 365 m 337 – 350 m	1 (Very Low) 2 (Low) 3 (Moderate) 4 (High) 5 (Very High)	Low topographic depressions collect and store regional surface runoff.
Soil Texture	4.76%	Arenosols (Sandy Loam) Fluvisols (Clay / Silty Clay)	2 (Low) 5 (Very High)	Fluvisols possess low hydraulic conductivity, causing saturation.
Land Use / Land Cover	4.76%	Dense Vegetation Shrubland Bare Surface Farmland Built-up / Water Body	1 (Very Low) 2 (Low) 3 (Moderate) 4 (High) 5 (Very High)	Built-up areas increase imperviousness; farmlands reduce infiltration.

Author's Compilation, 2021

Analytic Hierarchy Process (AHP) weighting and consistency verification

The Analytic Hierarchy Process (AHP), pioneered by Saaty (1980), was employed to determine the relative importance weights of the conditioning criteria. A pairwise comparison matrix was constructed based on Saaty's standard 1–9 fundamental scale (Table 3).

To ensure logical transitivity and mathematical validity, the Consistency Ratio (CR) was evaluated using Equations (i) and (ii):

$$CI = (\lambda_max - n) / (n - 1) \quad \text{(i)}$$

$$CR = CI / RI \quad \text{(ii)}$$

where CI is the Consistency Index, λ_max is the principal eigenvalue, n is the number of criteria evaluated (n = 5 composite criteria), and RI is the Random Inconsistency Index derived for matrix order n (Table 4). Saaty established that a CR value < 0.10 indicates acceptable matrix consistency, whereas CR ≥ 0.10 necessitates revision of pairwise comparisons.

Table 3: Saaty's 1–9 Fundamental Pairwise Comparison Scale

Relative Importance	Definition	Qualitative Explanation
1	Equal importance	Two criteria contribute equally to the objective.
3	Moderate importance	Experience and judgment slightly favor one criterion over another.
5	Strong importance	Experience and judgment strongly favor one criterion over another.
7	Very strong importance	A criterion is favored very strongly over another; its dominance demonstrated in practice.
9	Extreme importance	The evidence favoring one criterion over another is of the highest possible order of affirmation.
2, 4, 6, 8	Intermediate values	Compromise values between adjacent scale judgments.

Adopted from Saaty, (1994)

Table 4: Random Inconsistency Index (RI) Values for Matrix Orders 1 to 15

Number of criteria	1	2	3	4	5	6	7	8	9	10	11	12	13	14	15
RI	0	0	0.58	0.90	1.12	1.24	1.32	1.41	1.45	1.49	1.51	1.48	1.56	1.57	1.59

Adopted from Saaty (1997). For matrix order n = 5, RI = 1.12.

Multi-criteria weighted overlay modeling

The final Flood Susceptibility Index (FSI) was computed on a cell-by-cell basis across the study axis using weighted raster overlay (Equation 3):

$$FSI = \sum [i=1 \text{ to } n] (W_i \times S_i) \quad \text{(iii)}$$

where W_i represents the normalized AHP weight assigned to conditioning factor i (∑ W_i = 1.0), and S_i represents the standardized susceptibility score (1 to 5) of factor i. The resulting continuous FSI grid was categorized into three discrete flood susceptibility classes—Low, Moderate, and High Susceptibility—using the Natural Breaks (Jenks) optimization algorithm in ArcGIS 10.8.

Results and discussions

Topographic controls

4.1.1 Elevation: The Digital Elevation Model (DEM) reveals that surface elevations along the Hadejia River axis range from 337m to 419m above mean sea level (Figure 4). The terrain demonstrates a pronounced southwest-to-northeast downward gradient. High elevations (399–419m) dominate the southwestern interfluves in Miga and Kafin Hausa LGAs, functioning as topographic shedding zones that generate and export surface runoff. Conversely, low elevations (337–365m) characterize the northeastern floodplains across Guri, Kirikasama, Hadejia, and Malam Madori LGAs. Runoff generated in upstream catchments drains toward these low-lying floodplains, where minimal hydraulic gradients impede channel conveyance and induce extensive backwater flooding and overland inundation. Oriola & Bolaji (2012) noted similar observation in a part of Ilorin metropolis, Kwara state as they reported decreasing nature of the elevation of the floodplain had a direct implication of speed, intensity and erosive capacity of the water flood along the plain. In this same vein, similar experience of areas of lower elevations being at high risk of flood was reported by Njoku *et al.* (2013) in Aba metropolis, Nigeria.

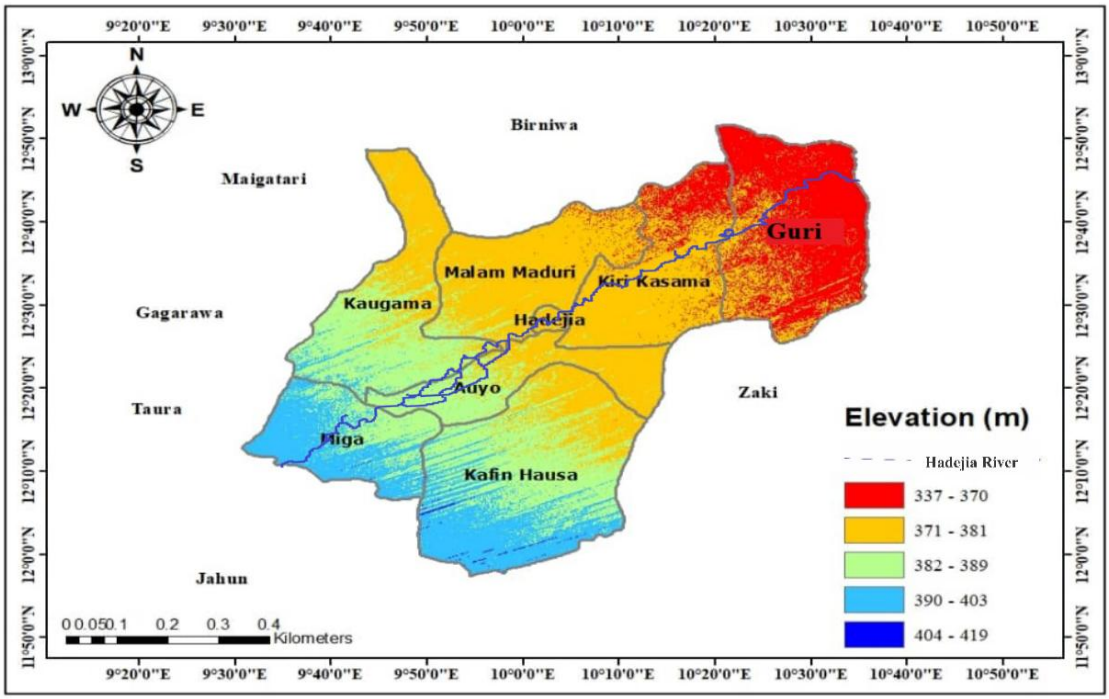


Figure 4: Digital Elevation Model (DEM) of the study area

4.1.2 Slope Gradient: The slope gradient map (Figure 5) exhibits values ranging from 0.00° to 49.5°, reclassified into five discrete susceptibility classes. The vast majority of the river axis is characterized by nearly level to very gentle terrain (0.00°–1.33°). Scientifically, slope gradient governs surface runoff velocity and gravitational drainage. Lower slopes retard overland flow velocity, diminishing the discharge capacity of sheet flow and promoting prolonged water stagnation and ponding during high-discharge periods. The northeastern LGAs (Guri, Kirikasama, Malam Madori, and Hadejia) are heavily dominated by these low slope gradients, significantly amplifying their physical susceptibility to prolonged inundation. In contrast, higher slope gradients (>5.8°) in portions of Miga and Kafin Hausa facilitate rapid gravitational evacuation of floodwaters, rendering these terrains substantially less susceptible. This finding is in line with that of Ogbonna *et al.* (2015) who reported that low slope areas are flood prone, moderate slope areas are less prone to flooding while high slope areas are flood free in Aba Urban, South-eastern Nigeria.

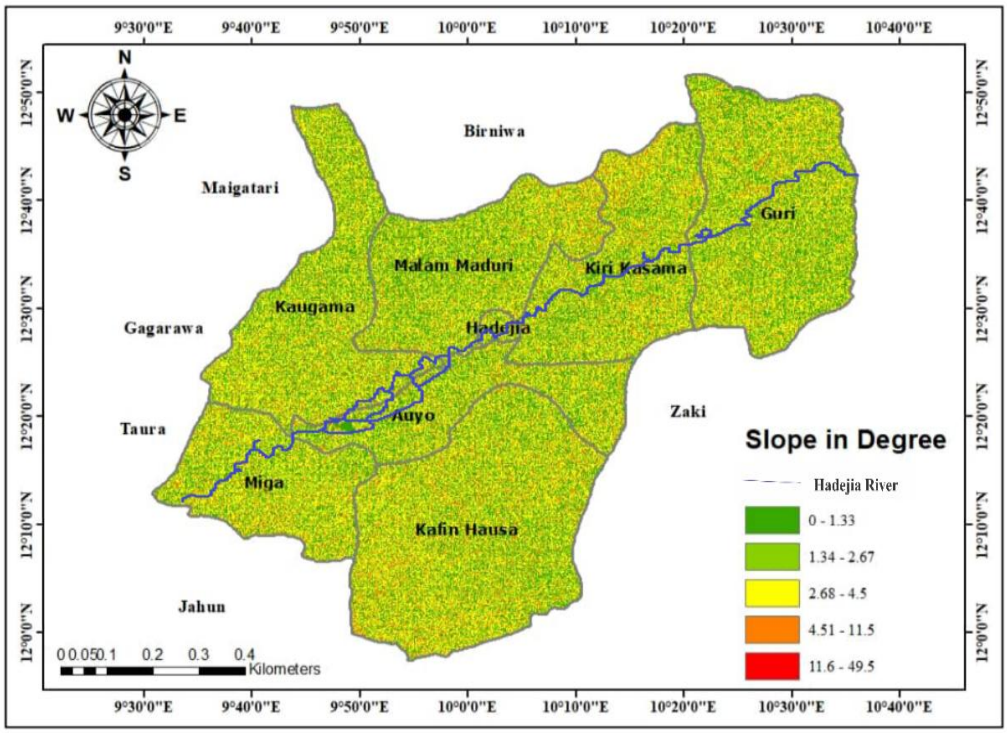


Figure 5: Slope Gradient map of the study area

Pedologic and climatic conditioning

4.2.1 Soil Texture: Spatial pedologic analysis delineates two principal soil units within the river axis (Figure 6): Arenosols and Fluvisols. Arenosols—predominantly coarse sandy loams—are characterized by high hydraulic conductivity and rapid infiltration capacity, significantly reducing surface runoff accumulation. These permeable soils occur primarily across elevated upland terraces in Malam Madori, Kaugama and Kafin Hausa LGAs, which are categorized as low flood susceptibility zones (Ernst, 2000). In sharp contrast, Fluvisols—comprising alluvial clay, silty clay and clay loams—dominate the low-lying active floodplains in Guri, Kirikasama, Auyo, Hadejia and southern Miga LGAs. Owing to their high clay content, fine pore structure, and high-water table, Fluvisols possess very low hydraulic conductivity and rapid saturation potential, inducing rapid saturation-excess surface runoff and extended inundation. This is in line with the findings of Shuaibu (2020) which indicates that Hadejia River Basin is characterized with sandy loamy and sandy clay having low infiltration rate which renders the region more prone to flooding hence having highest hazard.

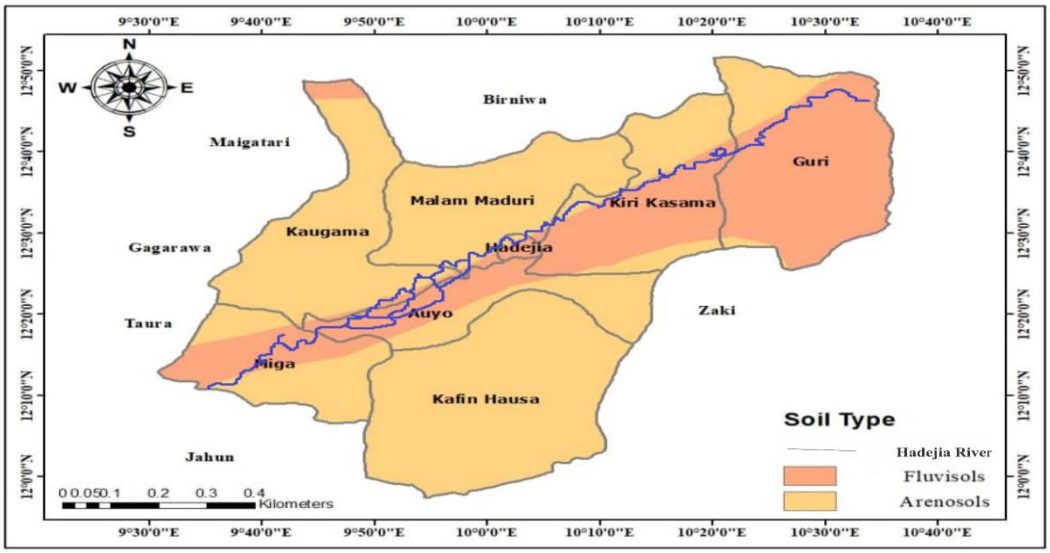


Figure 6: Soil Texture classification map of the study area

4.2.2 Precipitation Isohyets: The mean annual rainfall across the axis varies between 349 mm and 956 mm (Figure 7). Precipitation follows a strong regional climatic gradient, decreasing progressively from south to north under the controlling influence of the Inter-Tropical Convergence Zone (ITCZ). The highest precipitation totals (711–956 mm) are concentrated across southern LGAs (Miga, Kafin Hausa, and southern Auyo), generating substantial initial runoff volumes. Intermediate rainfall totals (591–710 mm) characterize central LGAs including Hadejia and Kaugama, while the northernmost reaches in Kirikasama and Guri receive lower local rainfall totals (349–470 mm). However, despite lower localized rainfall, the downstream LGAs receive concentrated channel flow routed from higher-rainfall upstream catchments, creating severe overbank inundation. This finding is in line with that of Shuaibu (2020) who found that high rainfall amount was received in the southern part of Hadejia river basin which increase the chance of flood events in this region.

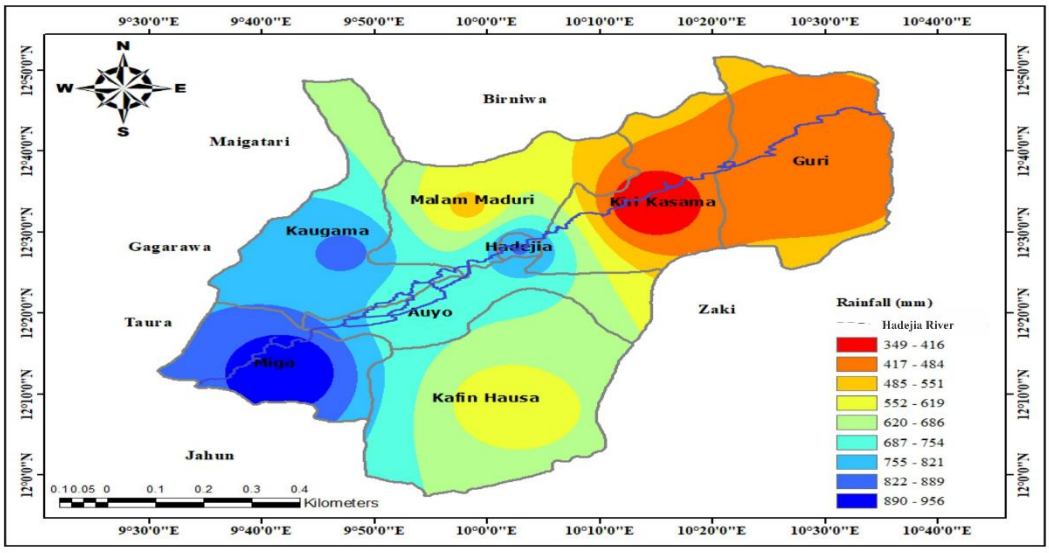


Figure 7: Mean Annual Rainfall Map of the study area (2011-2020)

Hydrographic factors

4.3.1 Drainage Density: Drainage density across the axis ranges from 7.07 to 132.0 km/km^2 (Figure 8). Very high drainage densities (108.0–132.0 km/km^2) and high densities (81.8–107.0 km/km^2) occur predominantly in agricultural floodplains and urbanizing clusters in Miga, Guri, Kafin Hausa, and Kirikasama. High drainage density signifies a densely branched channel network that rapidly collects surface runoff, concentrating high peak flows within short response times (Mahmoud & Gan, 2018). Lower drainage density classes (7.07–56.8 km/km^2) coincide with permeable shrubland interfluves.

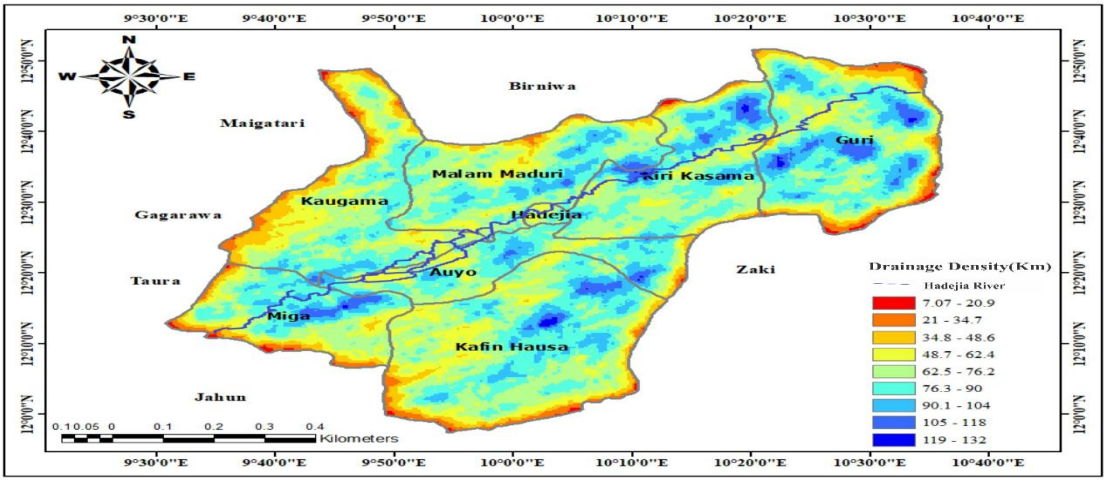


Figure 8: Drainage Density map of the study area

4.3.2 Channel Proximity: Euclidean distance buffering from the active river network (Figure 9) indicates that riparian flood susceptibility diminishes progressively with increasing distance from the channel. Terrains located within 1.0 km (<1,000 m) of the river channel are rated as Very High Susceptibility, directly exposed to initial channel overtopping and high-velocity scour. Areas between 1.0–2.0 km and 2.0–3.0 km are rated High and Moderate Susceptibility, representing active floodplain storage zones during seasonal bankfull exceedances. Distances exceeding 4.0 km exhibit Very Low susceptibility to fluvial flooding. This finding is in line with that of Umaru & Adedokun (2020) who found that areas within 6km buffer from the river Benue are most vulnerable to flood hazard than areas found within 13km buffer to River Benue of Kogi State. It is also in line with the findings of Kura *et al.* (2022) who reported that areas that falls within 250m from the drainage network are more susceptible to flooding that those at 500m away in Dutse, Jigawa state.

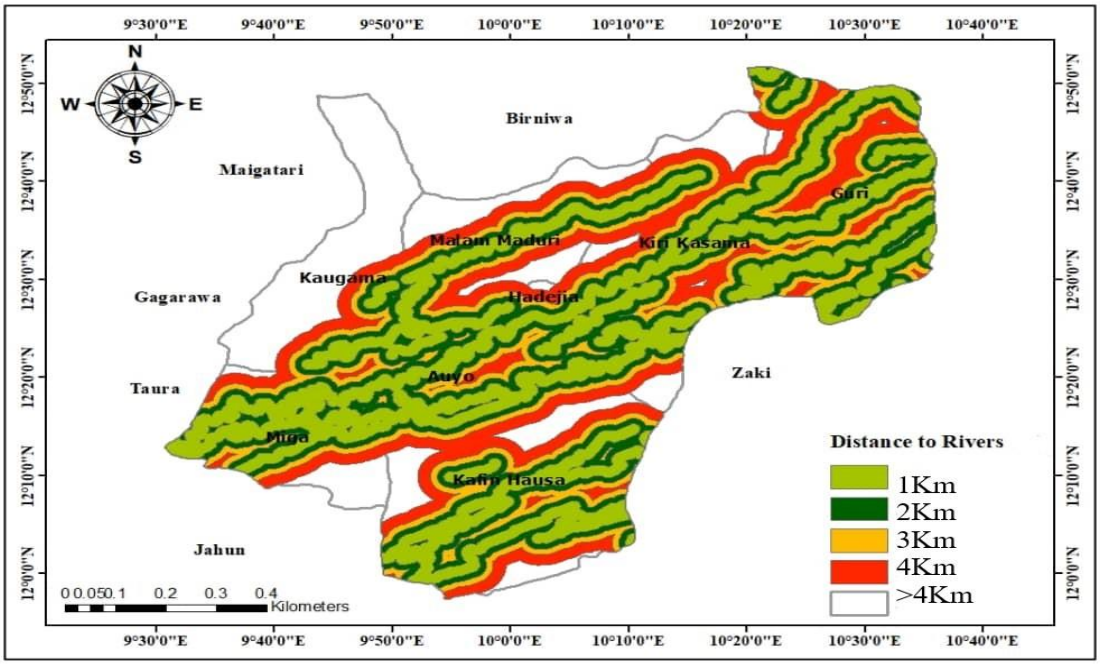


Figure 9: Distance to rivers map of the study area

Land use / land cover (LULC) spatial distribution

Spatial classification of Landsat 8 OLI imagery delineates six discrete LULC categories across the 0–5 km buffer axis (Figure 10; Table 5).

Table 5: Land Use / Land Cover (LULC) Classification and Area Metrics along the 0–5 km River Axis

LULC Classification Class	Area Extent (Hectares)	Proportion of Axis (%)	Environmental Characteristics & Hydrologic Influence
Shrubland	499,822.40	84.68	Semi-arid scrub and grassy interfluves with moderate infiltration.
Farmland	71,992.57	12.20	Rainfed cultivation and irrigated fadama floodplains.
Dense Vegetation	8,608.67	1.46	Riparian wetland woodlands, Typha grass beds, and thickets.
Built-up Areas	4,765.40	0.81	Impermeable rural and urban settlements, road infrastructure.
Water Bodies	4,739.61	0.80	Active river channels, perennial oxbow lakes, and reservoirs.
Bare Surfaces	326.47	0.06	Exposed sandy tracts, eroded banks, and compacted hardpans.
Total Study axis	590,255.12	100.00	Verified spatial domain of the 0–5 km river buffer axis.

Author's analysis, 2021

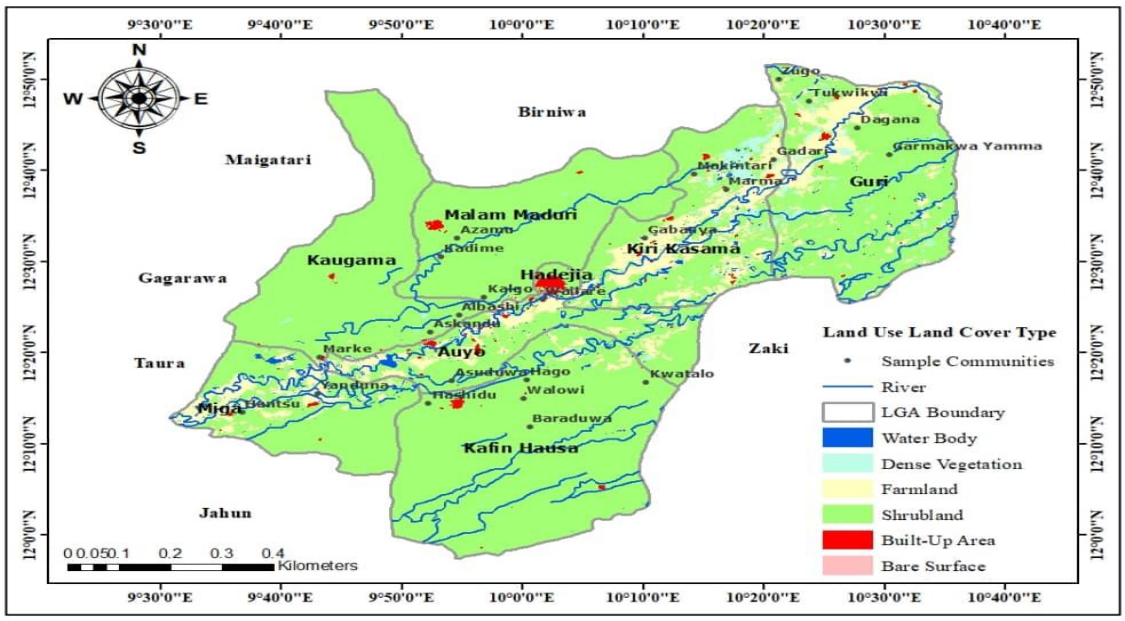


Figure 10: Land Use Land Cover (LULC) Map of the study area

Shrubland is the dominant surface cover, occupying 499,822.40 hectares (4,998.22 km^2; 84.68% of the axis). Shrublands provide natural soil cover that retards sheetwash runoff. Agricultural land constitutes the second largest cover type, spanning 71,992.57 hectares (719.93 km^2; 12.20%). Farmland is concentrated along the active alluvial riverbanks where soils are repeatedly cultivated for rice and wet-season crops. Agricultural tillage, ridging, and vegetation clearance modify natural infiltration, increasing vulnerability to overland flooding (Bello & Jeb, 2014). Dense vegetation and typha wetlands cover 8,608.67 hectares (86.09 km^2; 1.46%), while built-up areas occupy 4,765.40 hectares (47.65 km^2; 0.81%). Although settlements represent a small percentage of total area, their high impermeability and population density create critical focal points for flood damages. Open water bodies encompass 4,739.61 hectares (47.40 km^2; 0.80%) and bare surfaces comprise 326.47 hectares (3.26 km^2; 0.06%). This finding is contrary to that of Bello & Jeb (2014) who found the highest area extent of land use land cover of Birnin Kebbi to be within the Farmland area (59%) therefore making it more susceptible to flood.

AHP multi-criteria weighing

The multi-criteria weighting derived through the Analytic Hierarchy Process established mean annual rainfall as the most dominant conditioning factor (46.66%), followed by proximity to river channels and drainage density (26.86%), topographic controls of slope and elevation (16.97%), and surface characteristics of soil texture (4.76%) and LULC (4.76%) (Table 6). This hierarchical structure reflects expert consensus that within the semi-arid Sudano-Sahelian zone, monsoon precipitation depth serves as the primary meteorological driver generating the runoff volume that overwhelms seasonal channel storage (Rincón *et al.* 2018; Li *et al.* 2019).

However, spatial analysis reveals that while rainfall provides the hydrologic volume, hydro-geomorphic factors govern the localized concentration and duration of inundation. In the downstream reaches of Guri and Kirikasama, local annual rainfall totals are the lowest in the

axis (349–470 mm), yet these areas exhibit the highest physical flood susceptibility. This apparent paradox is explained by regional drainage mechanics: extreme precipitation occurring in upstream catchments (Kano and southern Jigawa) generates immense flood pulses that propagate downstream through the low-gradient Hadejia River. When these discharges reach the flat, clayey floodplains of Guri and Hadejia, the lack of hydraulic slope and high channel siltation cause massive overbank spilling, proving that terrain geomorphology and channel proximity govern local flood exposure.

Table 6: Analytic Hierarchy Process (AHP) Pairwise Comparison Matrix and Derived Factor Weights

Criteria	Rainfall	Distance / Drainage	Slope / Elevation	LULC	Soil Texture	Normalized Weight (W_i)	Rank
Mean Annual Rainfall	1.0000	3.0000	3.0000	7.0000	7.0000	46.66% (0.4666)	1
Distance to River /Drainage Density	0.3333	1.0000	3.0000	5.0000	5.0000	26.86% (0.2686)	2
Slope / Elevation	0.3333	0.3333	1.0000	5.0000	5.0000	16.97% (0.1697)	3
Land Use / Land Cover (LULC)	0.1429	0.2000	0.2000	1.0000	1.0000	4.76% (0.0476)	4
Soil Texture	0.1429	0.2000	0.2000	1.0000	1.0000	4.76% (0.0476)	5
Total Normalized Weight	—	—	—	—	—	100.00% (1.0000)	—

Expert Judgement,2021

Consistency diagnostics: λ_max = 5.2453, CI = 0.0613, CR = 0.0547 (CR < 0.10 confirms acceptable consistency). All weights sum to 100.0%.

Mathematical calculation for the 5 × 5 comparison matrix yielded a maximum eigenvalue λ_max = 5.2453. With n = 5 and RI = 1.12, the Consistency Index is CI = (5.2453 - 5) / (5 - 1) = 0.0613, resulting in a Consistency Ratio CR = 0.0613 / 1.12 = 0.0547 (5.47%). Because CR < 0.10, the pairwise judgment matrix exhibits robust mathematical consistency.

Flood susceptibility zonation across the Hadejia River axis and the 23 communities

Integration of the standardized thematic raster layers via weighted overlay produced the comprehensive Flood Susceptibility Map of the Hadejia River axis (Figure 11). Using the Natural Breaks (Jenks) classification method, the study axis was partitioned into three distinct flood susceptibility classes: High, Moderate and Low Susceptibility (Table 7).

Table 7: Delineation of Flood Susceptibility Classes and Distribution across the Eight Target LGAs

Susceptibility Class	Axis Area (ha)	Percentage (%)	Primary Affected LGAs	Dominant Hydro-Geomorphic Characteristics
High Susceptibility	218,534.18	37.02	Guri, Hadejia, Auyo, southern Kirikasama, eastern Miga	Low elevation (337–365 m), flat slope (0°–1.33°), Fluvisols, river buffer <1–2 km, high drainage density.
Moderate Susceptibility	242,381.97	41.06	Malam Madori, central Miga, northern Kaugama, Kafin Hausa	Intermediate elevation (366–380 m), moderate slope (1.4°–5.7°), mixed Arenosol-Fluvisol transitions, 2–4 km buffer.
Low Susceptibility	129,338.97	21.92	Upland Kafin Hausa, western Kaugama, northern interfluves	High elevation (381–419 m), steeper slopes (>5.8°), permeable Arenosols, buffer >4 km, low drainage density.
Total Axis	590,255.12	100.00	Eight Local Government Areas	Complete integrated multi-criteria axis assessment.

Author's analysis

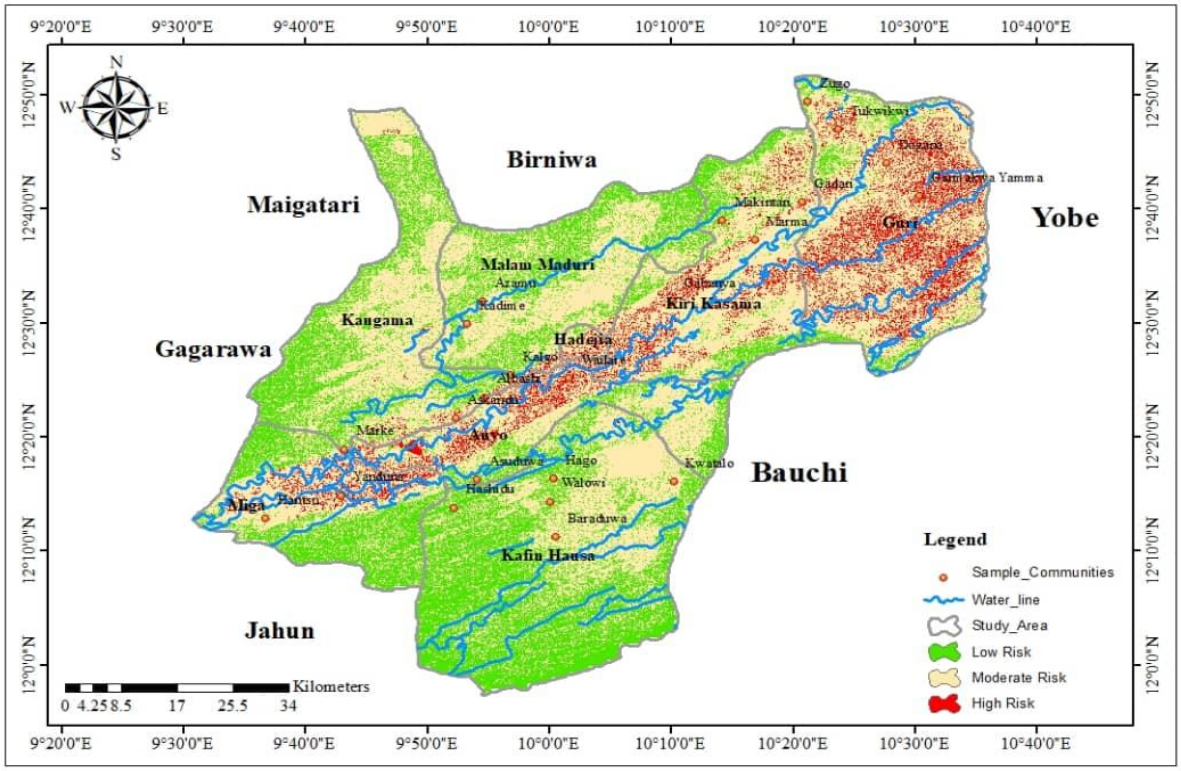


Figure 11: Composite Flood Susceptibility map along the study area

High Susceptibility zones cover 2,185.34 km^2 (37.02% of the axis). These zones are strongly concentrated along the contiguous riparian floodplain of Guri, Hadejia, Auyo and southern Kirikasama LGAs, as well as downstream reaches of Miga. The spatial co-occurrence of low elevations (337–365 m), nearly flat topography (0.0°–1.33°), poorly drained alluvial Fluvisols, high drainage density (>81.8 km/km^2) and immediate proximity to the river channel (<1–2 km) creates severe exposure to seasonal overbank spilling. Among the 23 farming communities mapped in this study, 14 settlements fall directly within this High Susceptibility zone.

Moderate Susceptibility zones span 2,423.82 km^2 (41.06% of the axis), forming an intermediate transitional belt across Malam Madori, central Miga, northern Kaugama and portions of Kafin Hausa. These areas experience inundation during extreme, high-return-period flood events or following prolonged upstream dam discharges. Seven of the 23 farming communities are situated within this intermediate zone.

Low Susceptibility zones encompass 1,293.39 km^2 (21.92% of the axis), occupying the elevated southwestern interfluves of Kafin Hausa and western Kaugama. These areas feature elevations above 381 m, slopes exceeding 5.8°, porous Arenosol soils and buffer distances >4.0 km from the main river channel. Two communities located on high terraces fall within this zone.

Implications for smallholder agrarian risk management

The delineation of flood susceptibility along the Hadejia River axis carries profound practical implications for agricultural disaster management in Jigawa State. With over 80% of the axis occupied by smallholder farmlands and communal grazing, the concentration of High Susceptibility across 14 of the 23 farming communities explains the catastrophic crop losses documented during recent flood disasters. Because smallholder farmers depend on

seasonal fadama cultivation for subsistence and income, persistent flooding traps agrarian households in cycles of debt and asset depletion.

Conclusion and recommendations

Conclusion

This study developed a high-resolution, GIS-based multi-criteria flood susceptibility model along the Hadejia River axis in Jigawa State, evaluating seven hydro-geomorphic conditioning factors across a 0–5 km buffer zones covering 5,902.55 km^2 (590,255.12 hectares) and anchored by 23 farming communities. The Analytic Hierarchy Process (AHP) established a mathematically consistent criteria weighting structure (CR = 0.0547 < 0.10) that accounted for all five evaluated criteria, led by mean annual rainfall (46.66%), distance to river and drainage density (26.86%), slope and elevation (16.97%), soil texture (4.76%), and land use/land cover (4.76%).

Weighted raster overlay delineated the axis into High (37.02%), Moderate (41.06%) and Low (21.92%) flood susceptibility classes. High-susceptibility zones are heavily concentrated across Guri, Hadejia, Auyo, southern Kirikasama, and eastern Miga LGAs, where low elevations (337–365 m), flat terrain (0°–1.33°), poorly drained alluvial Fluvisols, high drainage density and river proximity (<1–2 km) converge to create severe overbank inundation hazards. Fourteen of the 23 farming communities fall within this high-hazard belt. These findings confirm that while seasonal rainfall provides the hydrologic volume, localized geomorphology and channel proximity govern inundation severity.

Recommendations

Based on the empirical findings, the following recommendations are offered for policy, environmental planning and flood mitigation:

1. Adoption of Susceptibility Maps in Spatial Planning: The Jigawa State Ministry of Environment, State Emergency Management Agency (SEMA) and National Emergency Management Agency (NEMA) should utilize the high-resolution susceptibility mapping as a baseline spatial screening tool for flood hazard mitigation and infrastructure planning.
2. Targeted Channel Desilting and Typha Grass Clearance: River management authorities should prioritize targeted hydraulic dredging and clearance of invasive Typha domingensis grass along high-susceptibility choke points in Guri, Hadejia, and Auyo to restore bankfull conveyance capacity.
3. Agricultural Flood-Resilience Interventions: Agricultural extension services and rural development agencies should introduce flood-tolerant cereal varieties, promote crop insurance mechanisms, and establish early-warning dissemination networks tailored to the 14 highly susceptible riparian farming communities.
4. Land-Use Regulation and Buffer Protection: Local Government Authorities should enforce zoning regulations that restrict permanent residential expansion within the high-hazard 0–1 km river buffer zone while preserving natural floodplains for controlled agricultural recession farming.

5. Empirical Multi-Temporal Inundation Validation: Future studies should integrate multi-temporal radar satellite imagery (Sentinel-1 SAR) and hydrodynamic hydraulic routing (HEC-RAS) to empirically validate susceptibility thresholds against recorded flood extents.

Declarations

Author contributions (CRediT): *Not applicable*

Funding: *Not applicable*

Conflict of interest: *Not applicable*

Ethics approval and consent (where applicable): *Not applicable*

Data availability: *Not applicable*

Use of AI tools (where applicable): *Not applicable*

Acknowledgements: *Not applicable*

References

Alfa, M. I., Ajibike, M. A., & Daffi, R. E. (2018). Application of Analytic Hierarchy Process and Geographic Information System Techniques in Flood Risk Assessment: A Case of Ofu River Catchment. *Journal of Degraded and Mining Lands Management*, *5(4)*, 1363–1372.

Anugwara, B. & Emakpe, G. (2013). Flood disasters and agricultural impacts in Nigerian river basins. Environmental Press, Lagos, Nigeria.

Bello, M.N. & Jeb, D.N. (2014). Analysis of Flood Risk Inundation Hazard in Birnin Kebbi Town, Kebbi State, Nigeria. *International Journal of Geomatics and Geosciences*, 5(1): 119-131.

Ernst, W. G. (2000). Earth Systems: Processes and Issues. Cambridge University Press, Cambridge, UK.

European Commission (EC) (2007). Directive 2007/60/EC of the European Parliament and of the Council of 23 October, 2007 on the assessment and management of flood risks. Official Journal of the European Union, L288/27-34. Available online at http://eurlex.europa.eu/LexUriServ/LexUriServ.do?uri=OJ:L:2007:288 :0027:0034:EN:PDF, last assessed November 20, 2020

Kura, N.U., Usman, S.U. & Khalil, M.S. (2022). Flood Vulnerability Assessment of a Semi-Arid Region: A Case Study of Dutse in Jigawa State, Nigeria. *Journal of Environmental Issues and Climate Change,* 2 (1): 20-30.

Li, W., Lin, K., Zhao, T., Lan, T., Chen, X., Du, H., & Chen, H. (2019). Risk assessment and sensitivity analysis of flash floods in ungauged basins using coupled hydrologic and hydrodynamic models. *Journal of Hydrology*, *572*(March), 108–120. https://doi.org/10.1016/j.jhydrol.2019.03.002

Mahmoud, S. H. & Gan, T. Y. (2018). Multi-criteria approach to develop flood susceptibility management along Hadejia River Basin, northwestern Nigeria. *H2Open Journal*, *2* (1), 184– 199. https://doi.org/10.2166/h2oj.2019.010

Mishra, K., & Sinha, R. (2020). Flood risk assessment in the Kosi megafan using multi-criteria decision analysis: A hydro-geomorphic approach. Geomorphology, 350, 106861.

Molinari, D., Menoni, S., & Ballio, F. (2017). *Flood Damage Survey and Assessment: New Insights from Research and Practice*. American Geophysical Union (AGU) & John Wiley & Sons. https://doi.org/10.1002/9781119217930

Njoku, J.D., Amangabara, G.T. & Duru, P.N. (2013). Spatial Assessment of Urban Flood Risks in Aba Metropolis, using geographical information systems techniques. *Global Advanced Research Journal of Environmental Science and Toxicology* 2 (3): 086–092.

Ogbonna, C.E., Ike, F. and Okwu-Delunzu, V.U. (2015). Spatial Assessment of Flood Vulnerability in Aba Urban Using Geographic Information System Technology and Rainfall Information. *International Journal of Geosciences*, 6(3): 191-200. http://dx.doi.org/10.4236/ijg.2015.63013

Oriola, E. & Bolaji, S. (2012). Urban risk information on river catchment in a part of Ilorin metropolis, Kwara State, Nigeria. Journal of Environment and Earth Science, 2(8), 70–83.

Rincón, D., Khan, U. T. & Armenakis, C. (2018). Flood risk mapping using GIS and multi criteria analysis: A Greater Toronto Area case study. *Geosciences*, *8*(8), 275.

Saaty, T. L. (1980). The Analytic Hierarchy Process: Planning, Priority Setting, Resource Allocation. McGraw-Hill International, New York.

Saaty, T. L. (1994). Fundamentals of Decision Making and Priority Theory with the Analytic Hierarchy Process. RWS Publications, Pittsburgh, PA.

Saaty, T. L. (1997). A scaling method for priorities in hierarchical structures. Journal of Mathematical Psychology, 15(3), 234–281.

Saaty, T. L. (2008). Decision making with the Analytic Hierarchy Process. International Journal of Services Sciences, 1(1), 83–98.

Shuaibu, A. (2020). Flood reduction through flood risk and vulnerability assessment and mapping in Hadejia River Basin, Nigeria. MSc Thesis, PAUWES, Tlemcen, Algeria.

Shuaibu, A., Hounkpe, J., Bossa, Y.A. & Kalin, R.M. (2022). Flood risk assessment and mapping in the Hadejia River Basin, Nigeria using Hydro-Geomorphic Approach and Multi-Criterion Decision Making method. *Water,* 14(22): 3693. Doi: 10.3390/w14223693

Swiss Re. (2020). Natural catastrophes in times of economic accumulation and climate change. Sigma Report No. 2/2020, Swiss Re, Zurich.

Umaru, E.T. & Adedokun, A. (2020). Geospatial analysis of flood risk and vulnerability assessment along River Benue of Kogi State. *Journal of Geographic Information System*, 12(1), 1-14.

Vishwanath, V. H., & Tomaszewski, B. (2018). Flood Hazard, Vulnerability and Risk Assessments for Uttarakhand State, India. Disaster Research Report, RIT, Rochester, NY.